Temperature induced mobility and recombination of atomic oxygen in crystalline Kr and Xe. I. Experiment

A. V. Danilychev and V. A. Apkarian
Department of Chemistry, University of California, Irvine, California 92717

(Received 20 July 1993; accepted 20 August 1993)

Recombinant molecular spectra of O_2 in crystalline Kr and Xe, obtained from sudden recombination induced by laser pumping of the predissociative B state, and by adiabatic recombination induced thermally, are reported. All electronic states that correlate with $O(^3P)+O(^3P)$ are populated by both methods in Kr. The excited triplet states are strongly perturbed in Xe. Laser induced fluorescence (LIF) spectra of atomic O are also reported. Two emissions are observed in Kr; one at 563 nm with a radiative lifetime of 11 μs, and another at 599 nm with a radiative lifetime of 1.4 μs. These are assigned to emissions from neutral $O(^1S)$ trapped in substitutional and interstitial octahedral sites, respectively. O atoms are generated *in situ* by photodissociation of either O_2 or N_2O. The subsequent thermally induced recombination of atoms is followed using LIF from atomic centers and molecular thermoluminescence. The recombination follows first order kinetics, from which it is inferred that atomic mobilities are characterized by long-range migration, with migration lengths of $\geqslant$300 Å. Site specific Arrhenius rate constants are extracted from the analysis of glow curves. Only two sites, interstitial and substitutional O_h, contribute to the glow curves in crystalline Kr. A third site is present in crystalline Xe. A broad distribution of activation energies is observed in vapor deposited matrices.

I. INTRODUCTION

The thermal mobility of atoms in cryogenic rare gas solids, although phenomenologically well established, has not been quantitatively characterized previously. The problem is of general interest as an example of defect diffusion in compressible solids, and as a generic model of adiabatic dynamics in many-body systems. In this paper we describe an experimental effort aimed at characterizing thermal mobility in crystalline Kr and Xe of an open shell atom, oxygen, which in the isolated atomic ground state assumes the ^3P configuration. A rather unexpected behavior is observed, namely, the thermally induced mobility of O atoms is characterized by long-range migration. To rationalize this finding, a microscopic model is suggested: thermally induced change in spin multiplicity, from "triplet" to "singlet," and subsequent migration on the singlet surface. The proposed model is supported by the potential energy surfaces of the system which will be presented in a subsequent paper.

In the present studies, O atoms are generated *in situ* by photolysis of O_2 or N_2O as precursors. The thermally induced mobility and recombination of O atoms is then followed by monitoring laser induced fluorescence from atomic O centers, and by thermoluminescence from O_2. Laser induced fluorescence (LIF) from isolated O atoms is most conveniently generated by accessing charge transfer states between the trapped O atoms and the particular rare gas host. This approach, and the spectroscopy of O/Xe was delineated in a prior publication,[1] and has been previously used by several authors in studies of photodissociation[2] and exciton induced dissociation of O precursors.[3,4] Thermoluminescence (TL) is a well developed tool in radiation dosimetry, which has been broadly used in dating applications.[5] The method has been useful in studies concerning defects and impurities in solids, and has previously been applied in our group for the study of ion-hole recombination in rare gas matrices.[6] In rare gas matrices, thermoluminescence resulting from diffusion controlled recombination of atomic fragments on electronically excited surfaces, has previously been reported from a variety of systems: O_2 (Refs. 7 and 8), NO (Ref. 7), CO_2 (Ref. 8), S_2 (Ref. 9), and SO (Ref. 10) are examples. The emphasis in these works has been mainly spectroscopic, making no attempt at the quantitative characterization of the recombination dynamics. We rely on complimentary thermoluminescence, and laser induced fluorescence measurements, to characterize atomic mobilities and recombination kinetics. The data can be treated by homogeneous kinetics, and rather unexpectedly, the recombination of O atoms fits first order kinetics even in highly diluted samples. The latter is the key in the characterization of the thermally induced mobility of atoms as long range. The experimental findings are presented here. An understanding of the adiabatic many-body potentials that arise from the interaction of the open shell oxygen atom with the closed shell rare gas atoms are clearly crucial for the interpretation of the observed dynamics. A treatment of these surfaces in the electrostatic nonadditive pair-potential limit which seems to capture the ingredients necessary to rationalize the observed dynamics will be presented in a subsequent paper.

II. EXPERIMENT

The experiments are performed in free standing polycrystalline solids, grown from premixed gas samples. Details of the method have previously been described.[11] Highly transparent crystals of 1 cm$\times$1 cm$\times$1 cm dimension are grown in a Pyrex mold, in contact with a cryotip, held at 15 K. A backing pressure of 200 Torr is used

during growth. The crystal mold is retracted after the tip temperature drops to its bottom value of 8 K. A closed cycle cryostat, enclosed in a UHV shroud is used. The shroud, and all deposition lines are evacuated with a turbomolecular pump. Care is taken to eliminate all contaminants both during gas manipulations and after growth of the crystal. The manifold base pressure is maintained below 5×10^{-7} Torr. The vacuum chamber around the cryotip is usually outgassed for 1 h at 10^{-8} Torr before cooling. With the cryostat at 8 K, a base pressure better than 5×10^{-10} Torr is maintained; at higher temperatures the chamber pressure is determined by the vapor pressure of the particular crystal. The deposition gas line is commonly passed through a dry-ice acetone bath in order to minimize contamination of the crystal with H_2O.

Accurate thermometry is crucial in these experiments. To accomplish this, two cross calibrated temperature sensors are used. An Au:Fe vs chromel thermocouple is embedded inside the crystal, while a factory calibrated Si diode of stated accuracy ±0.1 K (Lakeshore Cryotronics) is fixed on the cryotip. The absolute calibration is further tested by measuring the vapor pressure of crystal Ne as a function of temperature, near 8 K. The initial calibration was retained throughout the measurements. The temperature readout is accomplished by a personal computer through a GPIB connection. Precision of measurements, as gauged by the agreement between the two sensors, is better than 0.1 K, while the absolute accuracy is estimated to be within 0.2 K. Warm up of the crystal is accomplished with a resistive heater attached to the cryotip. To ensure homogeneous heating in measurements of glow curves (fluorescence intensity versus temperature or time), temperature ramp rates of 0.05 K s^{-1} are used with a data acquisition rate of 0.5–1 Hz. In the case of Xc, the temperature is typically cycled between 8 and 70 K. The sample retains its optical clarity throughout the cycle. Dispersed temperature induced fluorescence, from 300 to 850 nm, is recorded using an optical multichannel analyzer (Princeton Applied Research OMA3). Otherwise, glow curves are recorded with a PMT, through a 0.25 m monochromator, using a mechanical chopper and lock-in amplifier.

In both O_2 and N_2O doped solids, O atoms are photogenerated by irradiation of the samples at 193 nm. The photodissociation of N_2O in solid Xe at this wavelength has been demonstrated by Weitz *et al.* to proceed with near unit quantum efficiency.[12] The same is true in solid Kr. The 193 nm photodissociation of O_2 in rare gas solids is not fully understood. Despite the fact that the excitation wavelength falls between vibronic resonances in the $B\leftarrow X$ Schumann–Runge band,[13,14] intense recombinant emission is observed, indicating that the molecule is efficiently excited by the radiation. While the B state is known to be predissociative in the gas phase,[15] it does not lead to efficient cage exit of O atoms in the solid. Permanent dissociation occurs upon 193 excitation of O_2, as verified by observing LIF from O centers; however, this constitutes only $\sim1\%$ of the molecules, as verified by the near constancy of LIF from the molecular species. That only O_2 molecules at defect sites undergo dissociation, is a possibility that has not been rigorously established.

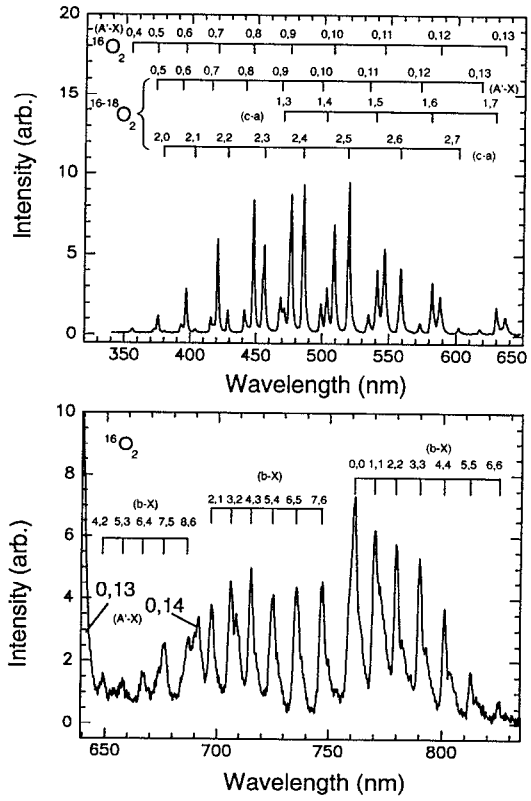

FIG. 1. 193 nm laser induced recombinant emission of O_2 in Kr (M/R = 10 000). Upper panel: $A'\rightarrow X$ and $c\rightarrow a$ emissions. Lower panel: $b\rightarrow X$ emission.

III. RESULTS

A. Molecular spectra

Laser induced emission spectra from O_2 doped solid Kr irradiated at 193 nm is shown in Fig. 1. The observed transitions can be unambiguously assigned. The emission centered around 750 nm, is due to $b(^1\Sigma_g^+)\rightarrow X(^3\Sigma_g^-)$ sequences, in good correspondence with the prior description of this band in Ar, by Schurath and co-workers.[16] The blue emissions can be assigned to $A'(^3\Delta_u)\rightarrow X(^3\Sigma_g^-)$ and $c(^1\Sigma_u)\rightarrow a(^1\Delta_g)$ Herzberg bands, in good agreement with the description of intensities and their dependence on temperature, and isotopic mixing given by Brus *et al.*[17] In that work, the spectra were obtained by direct resonant excitation into the $A'\leftarrow X$ bands near 260 nm. The excitation in our case leads to the predissociative $B(^3\Sigma_u^-)$ state, and the subsequent molecular fluorescence is due to geminate recombination on the various surfaces that correlate with the $O(^3P)+O(^3P)$ asymptotic limit. The agreement between the two sets of spectra, would imply that the partitioning of population between the nested A, A', and c potentials occurs deep inside the bound potentials, and has little memory of the mixing between states at the stretched molecular configuration reached by predissociation. While in the red spectral range we only observe emission from $b(^1\Sigma_g^+)$, the

presence of population in $a(^1\Delta_g)$ is also verified by measurements of emission intensity versus dark time between irradiation pulses.[18] We find that with continued irradiation at 193 nm, the $a(^1\Delta_g)$ with its lifetime of ~ 57 s,[18,19] acts as the main reservoir of population in O_2.

In effect, it can be deduced that all bound electronic states arising from $O(^3P)+O(^3P)$ are populated in this in-cage predissociation-recombination process.

After extensive irradiation of either O_2/Kr or N_2O/Kr samples at 193 nm, thermally induced fluorescence can be observed. The same spectrum is observed, independent of precursor. The observed thermoluminescence (TL) spectrum in Kr, is shown in Fig. 2 and compared with the LIF spectrum obtained under identical resolution, and at similar temperatures. The spectral distributions are quite similar. Clearly the same states are being observed, although the method of formation of O_2 is different: *sudden* in the case of LIF, and *adiabatic* in the case of recombination at thermal energies of ~ 30 K.

While in Ar and Kr, the observed molecular O_2 states are subject to only minor perturbations, in the case of Xe, the emission spectra are strongly degraded and the assignment of transitions in the Herzberg band region, is subject to controversy.[20,7,17(a)] In comparison to Kr, the emission intensity of the blue bands is greatly reduced in Xe, and strongly quenched at temperatures above 15 K. At lower temperatures, the 193 nm induced progressions can be clearly observed and assigned to the singlet $c \rightarrow a$ transition. An example of an LIF spectrum is shown in Fig. 3(a). Due to photodissociation, the $O_2(b \rightarrow X)$ emission in Xe is obscured by the strong continuous band of XeO. Given the difference in fluorescence lifetimes, 190 ns for XeO and ranging from 1–15 ms for the different vibrational levels in $O_2(b)$, the atomic and molecular emissions can be separated by appropriate gating, as shown in Fig. 3(b). The observed thermoluminescence in Xe is shown in Fig. 2(c). The contrast between Kr and Xe, as to the distribution of emission between blue and red bands, is apparent. While in Kr over 95% of the emission is in the blue, the opposite is true for the case of Xe. This, together with the observed degraded blue emissions under LIF, and very strong temperature dependent quenching of the Herzberg bands, are taken to imply that the A and A' triplet states of O_2 in Xe are strongly perturbed, and may be predissociative.

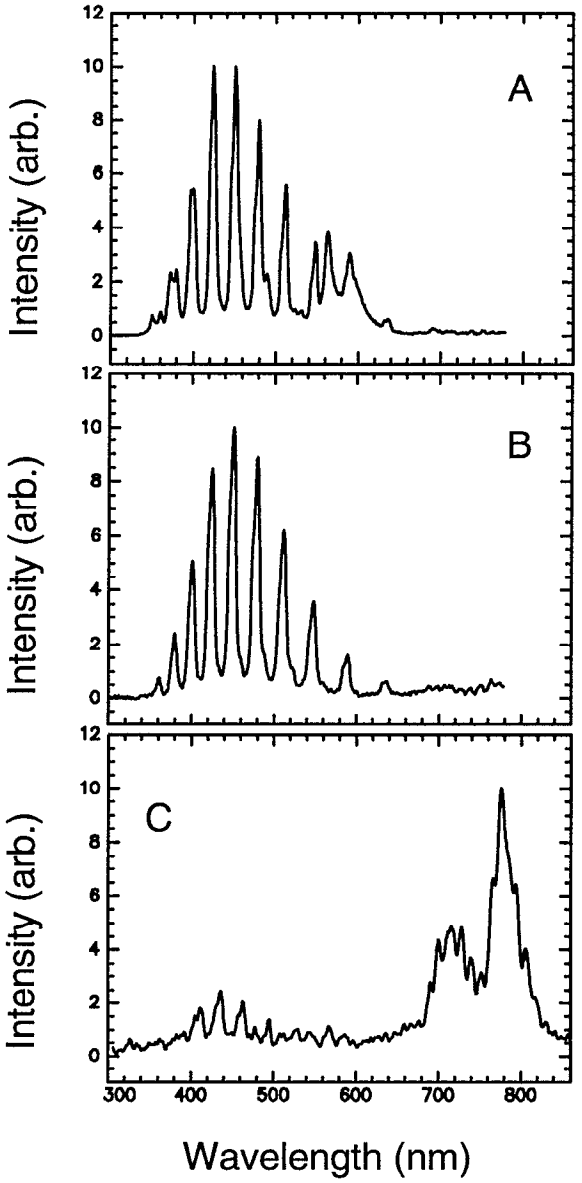

FIG. 2. Comparison of emission by sudden and adiabatic recombination of O_2. (a) O_2/Kr emission induced by 193 nm laser. The O/Kr bands are also observed at 563 and 599 nm ($M/R=10\,000$, $T=20$ K). (b) Thermoluminescence spectrum after dissociation of O_2 in the same sample as in (a), the spectrum is integrated over the temperature range of 28–30 K. (c) Thermoluminescence spectrum after dissociation of O_2 in Xe, original sample concentration of O_2:Xe=1:700, integrated over the temperature range of 35–40 K.

B. Atomic spectra

Both in Xe and Kr excitation at 193 nm produces emission from trapped O atoms. The O/Xe emission spectra have been previously described. They consist of two bands, one centered at 373 nm and another at 745 nm, which have been assigned to the diatomic $Xe^+O^-(3\,^1\Sigma^+) \rightarrow XeO(1\,^1\Sigma^+)$, $(1\,^1\Pi)$ parentage.[1] Both emissions decay with the upper state fluorescence lifetime of 190 ns at 15 K.

In O doped Kr prepared by photolysis of either O_2 or N_2O, 193 nm excitation leads to emission from two overlapping bands at 563 and 599 nm as illustrated in the first trace of Fig. 4. The 563 nm band decays with a fluorescence lifetime of 11 μs, while the 599 nm band decays with a lifetime of 1.4 μs. We also note that a broad emission centered at 595 nm with a lifetime of 115 ns due to XeO trapped in Kr also appears in this spectral range (see Fig. 4). Xe is a common contaminant in Kr, and the intense XeO emission can be mistaken for O/Kr. The two O/Kr atomic emissions were already reported in the early work of Shoen and Broida.[7] Taylor and Walker[3] identify them as "atomic" $O(^1S) \rightarrow O(^1D)$ at 563 nm, and "molecular" $2\,^1\Sigma^+ \rightarrow 1\,^1\Sigma^+$ at 599 nm, while Maillard *et al.*[21] assign them to the crystal field split states $^1A \rightarrow E_g$ and T_{2g}, respectively. While it is clear that both emissions are from O centers, the exact description of these transitions is lacking.

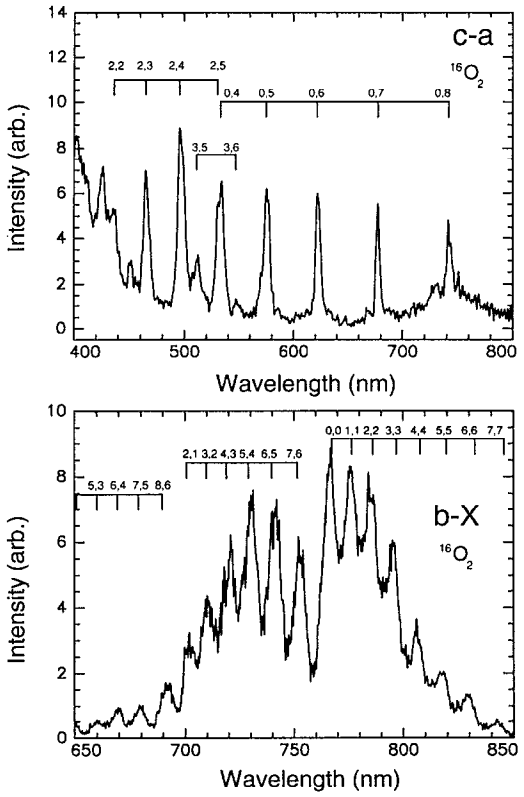

FIG. 3. 193 nm laser induced recombinant emission of O_2 in Xe (M/R =8000). Upper panel: Herzberg bands (sample at T=8 K). Lower panel: $b \rightarrow X$ emission (sample T=50 K). To avoid O/Xe emission, the PMT signal is boxcar integrated, with a delay of 1 ms, and a width of 20 ms.

The two emission bands have different thermal histories, and relative intensities that depend on precursor and photogeneration scheme.

When photogenerated from O_2 doped solids, the two peaks grow in simultaneously. When photogenerated from N_2O doped Kr, the 599 nm peak appears initially and only after extensive irradiation does a photochemical equilibrium get established between these two peaks. A spectrum obtained early in the photodissociation of N_2O in Kr, in which only the 599 nm peak can be observed is shown in Fig. 4. Upon warm up, the 599 nm peak is observed to disappear irreversibly at ~20 K, while the 563 nm peak disappears at ~30 K. Thus, the 563 nm peak can be isolated, also shown in Fig. 4, after a thermal cycle 8 K-20 K-8 K. As will be discussed later, the disappearance temperatures are directly correlated with O_2 thermoluminescence peaks. The two emissions can therefore be assigned to transitions from O atoms isolated in different lattice sites. They are likely to originate from mostly neutral states of $O(^1S)$/Kr, populated via predissociation of the ionic $Kr^+O^-(^1\Sigma^+)$ state.[1] This is consistent with the recent observation of emission from only ionic $Kr^+O^-(^3\Sigma^+)$ at ~5 eV in electron beam excited solids.[4] The 193 nm excitation overlaps with the tail of the Kr^+O^- charge transfer absorption band.[4] The observed lifetimes of 1.4 and 11 μs, which are much shorter than atomic $O(^1S)$ radiative lifetimes, are most likely due to the gain of oscillator strength by mixing with the ionic (Kr^+O^-) states. Based on this consideration alone, it would be expected that the shorter lifetime is associated with an atom trapped in a site much tighter than the atom emitting with the longer lifetime. Interstitial and substitutional trapping sites are the obvious possibilities.

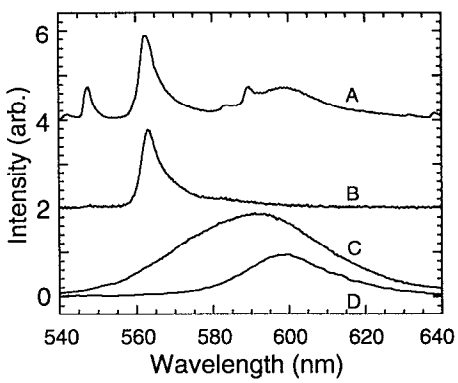

FIG. 4. Atomic emission spectra of O/Kr. Upper panel: Experimental spectra (a) 563 and 599 nm bands of O/Kr induced by 193 nm irradiation and additional lines due to molecular O_2 can be seen (M/R =10 000); (b) O/Kr emission from photodissociation of N_2O after heat cycle to 25 K; (c) XeO emission in Kr obtained by gating with 200 ns gate from a sample of initial composition N_2O:Xe:Kr=1:1:5000; (d) O/Kr emission early in the photodissociation of N_2O in Kr (M/R =10 000).

This is consistent with the simultaneous growth in these emissions when O_2 is the precursor, which would be expected to give a Frenkel defect by cage exit of only one of the O atoms. The assignment is also consistent with the observation of only interstitial O, early in the photodissociation of N_2O. The subsequent population of the substitutional site would therefore imply formation of substitutional trapping sites. N_2O would be expected to occupy a doubly substitutional site in these solids. Photogeneration of an interstitial O from N_2O would therefore leave behind a vacancy adjacent to the N_2 fragment. Extended irradiation could then either populate these vacancies by the photomobile O atoms, or alternatively, the lattice could relax around the photoexcited O atom by migration of the nearby vacancies.

C. Recombination

Glow curves in Kr are obtained by monitoring the 0-8 transition of $O_2(A' \rightarrow X)$ at 448 nm as a function of temperature. An example is shown in Fig. 5, from a sample with an initial N_2O:Kr ratio of 1:10 000. The formation of O_2 occurs at two different temperatures ~20 and ~30 K. These two TL peaks can be directly associated with the two emission bands observed in LIF of O/Kr. Upon a heat cycle 8 K-25 K-8 K, only the emission at 563 nm remains. The 599 emission disappears at 20 K. Disappearance of 563 nm emission occurs with the TL peak at 30 K. Upon subsequent irradiation, both emissions revert with relative intensities similar to that prior to heating. This establishes that the two emissions are from two different sites, with different barriers to recombination. The same glow curves,

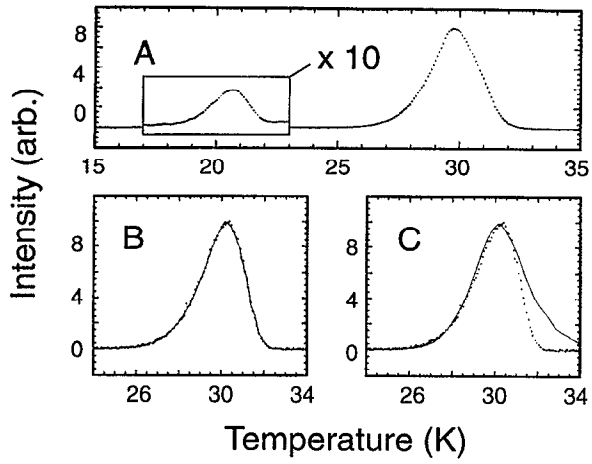

FIG. 5. Glow curve of O_2 in Kr. (a) shows two main peaks, at ~ 20.5 and ~ 30 K assigned to interstitial and substitutional sites, respectively. Initial concentration of the sample is $N_2O/Kr = 1{:}10\,000$; (b) first order fit of glow curve; (c) second order fit of glow curve.

with similar relative intensities under the two peaks, are obtained from samples varying in concentration from 1:700 to 1:30 000 of either O_2 or N_2O in Kr. The glow curves are not sensitive to extent of irradiation. These considerations are made to establish that the observed thermally induced formation of O_2 is not limited to geminate recombination, or reaction between pairs of atoms with correlated spatial distribution—the O_2 is formed among O atoms that are created with a random initial spatial distribution.

In the case of Xe, over 90% of the TL intensity is concentrated in the $b \rightarrow X$ band, with the brightest components being 0-0, 1-1, 2-2 [see Fig. 3(c)]. Since the entire TL spectrum is assignable to O_2 transitions, with the longest emission lifetime being ~ 15 ms, glow curves representative of the recombination kinetics could be recorded by monitoring total emission as a function of temperature. An example is shown in Fig. 6(a), taken from a sample of N_2O/Xe, at an initial concentration of 1:10 000. Three peaks, at 40, 47, and 61 K, contribute to the TL. The profiles of these curves are reproducible from sample to sample, within the precision of the temperature measurements of ± 0.2 K. The exception to this is the relative intensity of the 61 K peak, which seems sensitive to the crystal history. The observed peaks can be sharpened by partial annealing of the solid, which is accomplished by a heat cycle 8 K-32 K-8 K, prior to recording of the glow curve. An example is shown in the inset of Fig. 6(a). The partially annealed samples yield improved kinetic fits, and are regarded as the more reliable source of recombination rate constants.

Except for small variations in relative intensities, the peaks observed in the glow curves are highly reproducible in the free standing crystals. They clearly represent atoms trapped in reproducibly different trapping sites. Given that the majority of matrix isolation is conducted in thin films deposited on substrates at low temperature, a comparison of glow curves between the free standing crystal and a thin film matrix could yield information on site distributions of

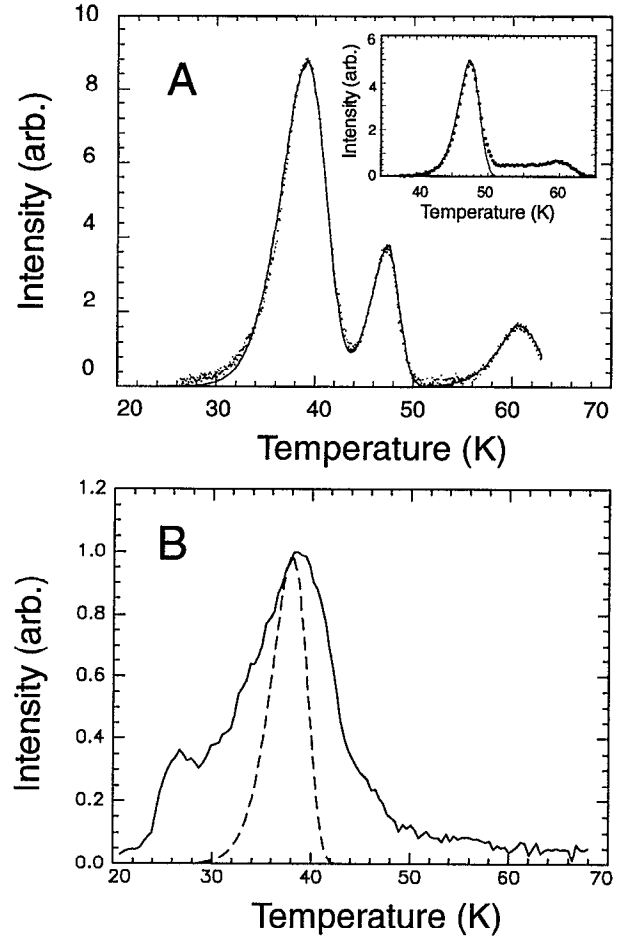

FIG. 6. Glow curve of O_2 in Xe. (a) Free standing crystal. The peaks are observed and fitted by first order kinetics. In the inset, isolation of the second peak is shown by initial thermal cycling. Original sample composition is N_2O:Xe 1:30 000. The deviation of the high temperature side of the fit in the inset from first order kinetics is used to estimate a lower limit to long range migration of 300 Å. (b) Glow curve from a pulse-deposited matrix. For the sake of comparison, the free standing crystal curve is included.

trapped atoms. We therefore carried out the same measurements in a pulse deposited matrix. The resulting glow curve is shown in Fig. 6(b). The glow peaks observed in the crystalline samples are buried in a broad distribution of sites. Quite clearly the glow curves are sensitive to the defects of the pulse-deposited matrix. No attempts were made to anneal the matrices, however, it was noted that repeated measurements on a given spot were not reproducible, nor were they reproducible from sample to sample.

The TL curves measure the formation rate of O_2 as a function of temperature. The same information should in principle be obtained by monitoring the disappearance of O atoms. This could be verified by monitoring LIF from XeO at 750 nm in Xe. The LIF method, in principle, has even higher sensitivity, however, it should be applied with caution since photoinitiated mobility of O atoms, recognized by Weitz *et al.*,[12] affects the observed TL profiles. For these measurements, the laser intensity is reduced by 3 orders of magnitude from its level used in photogeneration. Furthermore, it is verified by repeating measurements at different

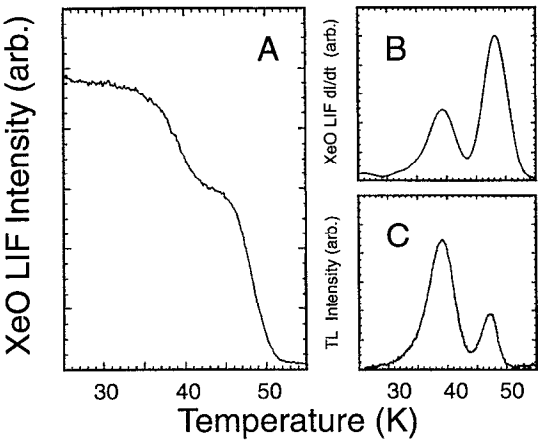

FIG. 7. Thermal recombination curves in Xe. (a) Temperature induced decay of LIF from O/Xe; (b) time derivative of (a); (c) glow curve. The curves in (b) and (c) yield identical kinetic fits however show different relative intensities. This is ascribed to differences in excitation cross sections of the two different sites. A linear temperature ramp of 0.05 K/s is used in these measurements.

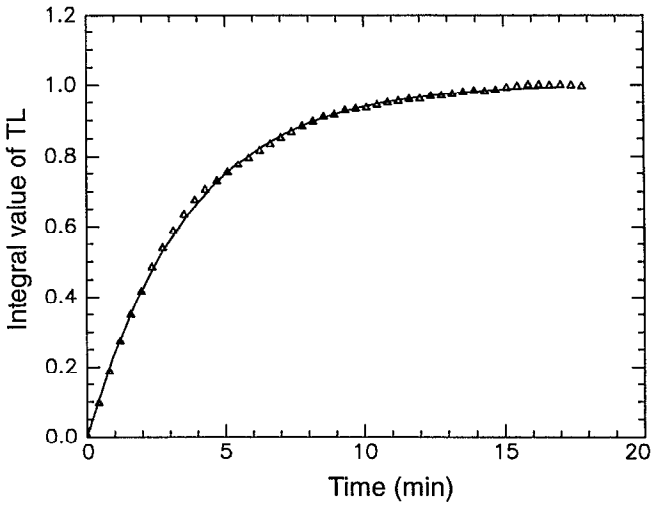

FIG. 8. Integral of isothermal glow from recombinant O_2 in Xe. The data is obtained at 37.4 K after an initial linear temperaure ramp (not shown). The curve is exponential. The fit, which is shown, yields a time constant of 215 ± 5 s. Every tenth point of the data is shown.

fluences that the obtained curve shapes do not depend on laser intensity or pulse repetition rate. An example of the decay of LIF from O atoms as a function of T, taken from a sample of N_2O/Xe with initial concentration of 1:10 000, is shown in Fig. 7(a). The intensity subsides stepwise, at the same temperatures at which TL peaks are observed. A direct comparison between glow curves and LIF loss curves is possible by differentiating the latter with respect to time. Such a comparison is made in Figs. 7(b) and 7(c). While the peak profiles obtained from these complimentary measurements are identical, the areas under the peaks are different. This difference is attributed to the difference in excitation cross sections of O atoms in different trapping sites. The observation of different TL peaks clearly implies that there are different trapping sites, with pronounced site effect on O atom mobility. However, in contrast with Kr, the O emission spectrum in Xe does not show obvious site splittings. While in both Kr and Xe 193 nm absorption is ascribed to neutral-to-ionic transition, in Kr the emission is assigned to neutral upper state while in Xe the emission is ascribed to the ionic upper state. Charge transfer absorptions should be site sensitive, since they involve solvated ionic potentials. The strongly Stokes shifted ionic emissions, which terminate on repulsive walls, need not be site sensitive.

The rate law governing the recombination is of primary interest in the analysis of these results. This can be most directly tested by TL measurements at constant temperature. This was executed in an N_2O/Xe sample of 1:30 000. After dissociation of N_2O at 193 nm, at 8 K, the temperature of the solid was raised to 37.4 K (2 K below the TL maximum), with a heating rate of 0.05 Ks^{-1}. The decay in TL was measured after stabilization of the temperature. Both the TL decay and its integral are exponential, the latter is illustrated in Fig. 8. Exponential decay at fixed temperature is a direct manifestation of first order kinetics. The decay constant, extracted from the exponential fit, is 215 ± 5 s. This decay rate is in perfect agreement with the rate constant extracted from the total glow curve analysis (see Sec. IV).

In multitrap systems, communication between traps can effect kinetic analysis. The accessibility of one trap from another can be tested by several different schemes. A partial test for this process was conducted as follows. In the 1:10 000 sample N_2O dissociation is completed at 8 K and the sample temperature is raised to 50 K. After 15 min in the dark at this temperature, the recombination of the low temperature trap sites should be complete. This is verified by noting that upon resuming irradiation at 193 nm, the LIF intensity is reduced to 12% of its original value at 8 K. With continued irradiation the LIF decays. The decay curve can be fit with a double exponential, as illustrated in Fig. 9. The main decay constant, 12 s, is within a factor of 2 of what would be expected for recombination from the low energy trap. Note, the 63 K trap would decay on a time scale of 1×10^4 s at this temperature. Quite clearly this trap site is depopulated by photo-activated mobility. The first exponential decay represents a process in which the photoexcitation leads to population of lower energy trap sites, from which thermal migration occurs. While the data is fit with double exponential, it is not clear that the second rate process is first order. When O atoms are highly depleted, photomobility could lead to second order migration of atoms. Such a mechanism has been observed, and documented by Ryan and Weitz.[12]

IV. DISCUSSION

A. Recombination rate law

Description of the thermally induced migration of O atoms in crystalline rare gas solids is our chief aim. The main experimental result in this respect is that the thermally induced recombination of trapped O atoms proceeds with first order kinetics. The experimental design is made

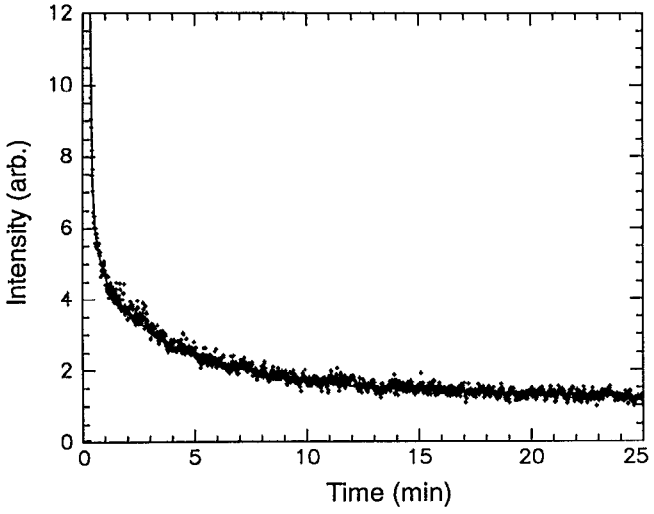

FIG. 9. Laser induced decay of LIF from atomic oxygen in Xe obtained after 15 min in the dark, at 52 K. The decay is fit by a double exponential with lifetimes of 0.132 ± 0.004 min and 4.22 ± 0.05 min.

to ensure that the initial O atom spatial distribution is random and, therefore, nongeminate recombination is being monitored. Moreover, this result is observed to hold at very large O:Xe dilutions, obtained by partial photodissociation of N_2O doped samples of $M/R = 30\,000$. The evidence for establishing the first order kinetics of recombination comes from three different measurements: (a) The kinetics of TL glow curves, which represent thermally induced recombinant emission from O_2; (b) the decay kinetics of O atoms probed by LIF as a function of temperature; (c) isothermal decay of the TL signal. The consistency of these complimentary measurements, coupled with the use of different O atom precursors, is the overwhelming evidence that proves the kinetics, and leads to the conclusion that the thermal mobility of O atoms is characterized by long-range migration. We quantify each of these points later.

The isothermal TL decay experiment at O atom dilutions greater than 1:30 000 yields itself to the most direct interpretation with respect to reaction order. After establishing that in Xe there are three main peaks in the TL curves, we ramp the temperature to the first peak and observe exponential decay, see Fig. 8. Therefore, the loss of O atoms, without specifying the final sink, obeys first order kinetics. This in itself is not sufficient to make conclusions about bulk mobility, since the possibility exists that the decay is due to geminate recombination. In all of our studies, O is photogenerated *in situ* from a precursor N_2O or O_2 and, therefore, if fragments remain near each other they may in principle undergo recombination without extensive migration. Geminate recombination would yield first order kinetics. Note, in the case of N_2O precursors, geminate recombination would imply recombination between $O(^3P)$ and N_2, a process that is activated by 1 eV in the gas phase and one that has previously been shown by IR studies not to occur in solids at cryogenic temperatures.[1,2] Nevertheless, reentry of O atoms into the original cage containing the N_2 fragment may lead to quenching of fluorescence and could therefore lead to decay of LIF with temperature.[1] Clearly, if the rate of O atom decay agrees with the rate of O_2 formation, in the same sample, in which N_2O is the precursor, then we can be confident that nongeminate recombination is being observed.

The loss of LIF from O and TL curves as a function of temperature were shown in Fig. 7 to be in excellent agreement. Quite clearly, both schemes measure the same process: the loss of nongeminate atom pairs. This observation, together with the exponential isothermal decay of O atoms is, in principle, sufficient to infer that the recombination of O atoms with a random initial spatial distribution proceeds via first order kinetics. Analysis of the glow curves further reinforce this conclusion.

Based on the profiles of the glow curves, it is possible to estimate that the observed kinetics is first order. In the case of linear temperature ramps, which is very nearly the case in most of our experiments, first order curves show a tail toward low temperatures, while second order curves show tails toward high temperature.[5] The asymmetry factor can be quantified by $M_g = (d_2/\Gamma)$ in which d_2 is the half width at half maximum (HWHM) on the high temperature side of the curve, and Γ is the full width at half maximum (FWHM). An $M_g = 0.42 \pm 0.03$ is observed in all the observed peaks in our studies. This is in agreement with the value of 0.430 ± 0.015 associated with first order kinetics, and outside the range for second order kinetics of 0.550 ± 0.015.[22] In all orders other than one, the TL curve shape will depend on the initial O atom concentration. We do not observe such a dependence. The TL curves from samples of very different initial precursor concentration, 1:600, 1:10 000, 1:30 000, are identical, and independent of extent of dissociation. Finally, both TL and LIF curves are well reproduced by first order kinetics, when the experimental temperature ramps are used in their analysis. Although the formalism for such treatments is well established, we restate the key steps.

The thermoluminescence intensity during a thermal ramp is proportional to the rate of formation of O_2 as a function of time;

$$I_{\mathrm{TL}}(t) \propto \frac{d[\mathrm{O}_2]}{dt} \tag{1}$$

while the LIF signal from an O atom in a given site, is directly proportional to the O atom concentration, weighted by the absorption cross section, σ, of a particular trap site,

$$I_{\mathrm{LIF}}(t) \propto \sigma[\mathrm{O}]. \tag{2}$$

As shown in Fig. 7, the negative derivative of the LIF loss curve follows the TL signal, i.e.,

$$I_{\mathrm{TL}}(t) \propto -\frac{1}{\sigma}\frac{dI_{\mathrm{LIF}}}{dt} \propto -\frac{d[\mathrm{O}]}{dt} \propto \frac{d[\mathrm{O}_2]}{dt}. \tag{3}$$

In first order kinetics

$$\frac{d[\mathrm{O}]}{dt} = -k[T(t)] \cdot [\mathrm{O}], \tag{4}$$

TABLE I. First order rate constants from thermoluminescence analysis.

Peak Temperature (K)	Activation Energy (K)	Frequency factor (Hz)
	Krypton	
20.5	614	3.7×10^{12}
30.5	909	5.1×10^{11}
	Xenon	
40.5	845	3.1×10^{7}
47.5	1490	5.6×10^{11}
61.0	1425	1.7×10^{8}

in which the time dependence of k, is through its dependence on temperature, $T(t)$. With the assumption of the Arrhenius form $k[T(t)]=\nu\exp[-E_a/k_BT(t)]$, and noting that

$$[\mathrm{O}]=-[\mathrm{O}]_0\cdot\exp\left(-\int_0^t k(\tau)d\tau\right) \tag{5}$$

the TL curve profile can be obtained as

$$I_{\mathrm{TL}}^{(1)}(t)\propto\exp\left(-\frac{E_a}{k_BT(t)}\right)\times\exp\left[-\nu\cdot\int_0^t\exp\left(-\frac{E_a}{k_BT(\tau)}\right)d\tau\right] \tag{6}$$

in which ν is assumed to be temperature independent.

To fit the TL data, ν and E_a are initially estimated based on the assumption of a linear T ramp. Then the exact experimental profile of $T(t)$ is used to numerically obtain the best fits. Where the peaks in the TL are well separated, as in the case of Kr, the fits are unambiguously good, see Fig. 5. In the case of overlapping peaks, we treat them as independent of each other, and again a rather good fit is obtained, see Fig. 6. It is also possible to isolate peaks by depleting low energy trap sites. This is shown for the case of the 47 K peak in Xe. The 40 K peak which overlaps it, is first depleted by raising the sample temperature to 35 K for $\sim$30 min. The temperature is subsequently ramped, and the glow curve of the isolated 47 K peak is recorded. The fitted parameters in these different methods are in good agreement. Each peak in the TL is then characterized by a frequency factor ν, and an activation energy, E_a; these are collected in Table I. Note, the extracted Arrhenius parameters of the first peak in Xe, yields a recombination time of 209 s at 37.4 K, in excellent agreement with the directly measured isothermal decay of TL at this temperature of 215 s (see Fig. 8).

Not withstanding the consistency of the treatments and the facts that the TL curves are well fit by first order kinetics and do not show any dependence on initial O atom concentration, we attempt second order fits to the data, to eliminate any ambiguity in the interpretation of the TL curves. For the second order mechanism of Eq. (9), it can be derived that the TL curves should be given by

$$I_{\mathrm{TL}}^{(2)}(t)\propto\exp\left(-\frac{E_a}{k_BT(t)}\right)\left\{1+\frac{\nu[\mathrm{O}]_0}{N}\times\exp\left[-\nu\int_0^t\exp\left(-\frac{E_a}{k_BT(\tau)}\right)d\tau\right]\right\}^{-1}, \tag{10}$$

where N corresponds to the concentration of trapping sites. The fit to this form for the well isolated TL peaks in Kr is shown in Fig. 5. Quite clearly, the curve is first order and not second order.

In summary, nongeminate recombination that can be well treated with first order kinetics is being observed, and the loss of O is directly matched with the formation of O_2.

B. Migration range

We consider the standard model for bimolecular recombination to clarify the implication of the finding of a first order rate law for recombination. O atoms isolated in the lattice are indefinitely stable with respect to recombination at temperatures below 10 K—a barrier prevents their mobility. Thermal excitation imparts mobility to atoms, by allowing them to overcome the barrier. Any barrier in the lattice is by definition periodic, and therefore the activated atoms, designated by O*, may retrap:

$$\mathrm{O}\xrightarrow{k_1}\mathrm{O}^*\xrightarrow{k_{-1}}\mathrm{O}. \tag{7}$$

At any given time, only a small fraction of the O atoms are expected to be activated and, therefore, the recombination should be dominated by the encounter of mobile atoms with the stationary ones:

$$\mathrm{O}+\mathrm{O}^*\xrightarrow{k_2}\mathrm{O}_2 \tag{8}$$

making the steady state assumption in O*, the disappearance of O atoms can be expressed as

$$\frac{d[\mathrm{O}]}{dt}=k_1\cdot k_2\cdot\frac{[\mathrm{O}]^2}{[\mathrm{O}]\cdot k_2+k_{-1}} \tag{9}$$

which reduces to a first order rate only if $k_2[\mathrm{O}]\gg k_{-1}$; i.e., if the rate of finding a stationary O atom is much larger than the retrapping rate constant. This is equivalent to the statement that first order kinetics arises if O* undergoes long-range migration. Specifically, the requirement is that the volume V swept by an activated atom prior to retrapping, $V=k_2/k_{-1}\gg1/[\mathrm{O}]$. At a dilution of 1:30 000, even if complete dissociation of the precursor is assumed, the condition implies that the swept volume is larger than 10^{-18} cm^3 or, equivalently, a migration range larger than 100 Å. Since first order kinetics persists for fractional dissociation the migration range should be significantly larger than this limit. As the O atom concentration drops due to recombination, the kinetics should, in principle, switch from first order to second order. Therefore, the deviation of the TL curve from a first order fit in the high temperature tail can be used as an estimate of the condition: $V=1/[\mathrm{O}]$. It can be seen in the inset of Fig. 6, that the first order fit accounts for more than 95% of the area under the curve. If there is a change in the rate law from first to second, it occurs

when O atom concentrations fall below 1 ppm. With this estimator, we can extract a migration range of ~ 300 Å. This rather surprising result rests on the observation of first order nongeminate recombination and the assumption of an initial statistical distribution of O atoms. The assumption of a statistical initial distribution of O atoms is based on IR studies, which establish that N_2O undergoes isolation in free standing crystals of Kr and Xe, but not in Ar.[11] The latter observation has prevented us from carrying the same studies in Ar.

C. Microscopic models

The microscopics leading to thermally induced long-range migration is not intuitively obvious. To see this, consider the periodic potential along the migration path of an interstitial $O(^3P)$ atom in a lattice at its equilibrium geometry. This can be estimated from ground state pair potentials which have been derived from molecular beam scattering data. The interaction of $O(^3P)$ with a $Rg(^1S)$ is angularly anisotropic, and splits into $^3\Pi$ and $^3\Sigma^-$ components.[23] Except for a shallow van der Waals well on the $^3\Pi$ surface, the interactions are essentially repulsive. As such, the ground state atom will be constrained to the largest cavities in the lattice. An interstitial atom will therefore be trapped in the O_h site, with six nearest neighbors. The largest window for exit from such a site is through the triangular, D_{3h}, faces of the octahedron. The exit leads to a T_d site, which, through another D_{3h} window is connected to a new O_h site. Thus, migration involves the O_h-T_d-O_h minimum energy path, with a barrier height determined by $V(D_{3h})$-$V(O_h)$. In the center of the O_h site, the P state is triply degenerate; while at the D_{3h} window it splits into P_z and $P_{x,y}$ components (perpendicular to, or contained in the plain of the triangle, respectively). Taking only nearest neighbors into account, it is easy to show that

$$\begin{aligned} V(O_h) &= 6V_0 = 2(V_\Sigma + 2V_\Pi), \\ V(D_{3h})_z &= 3V_\Pi, \\ V(D_{3h})_{x,y} &= \tfrac{3}{2}(V_\Sigma + V_\Pi), \end{aligned} \tag{10}$$

where V_0 is the isotropic term of the pair potential: $V_0 = (V_\Sigma + 2V_\Pi)/3$. Using the experimental gas phase pair potentials,[24] and for a rigid lattice, the barriers to migration of $O(^3P)$ in the rigid lattice are 1.4 and 1.25 eV in Kr and Xe, respectively. These barriers are more than an order of magnitude larger than the measured activation energies and cannot be overcome at thermal energies. Clearly the adiabatic dynamics of diffusion involves extensive lattice relaxation and the relevant barriers are not of potential but of free energy nature. Lattice relaxation can lower barrier heights, however, not sufficiently so to account for the observed energies. Moreover, if extensive lattice relaxation is required for atomic motion, then necessarily the migration would be characterized by hopping diffusion, i.e., retrapping at every lattice site. This picture would be similar to that of the self-diffusion of the lattice atoms, which is vacancy mediated and negligible at these temperatures.[24] Quite clearly, a special mechanism is to be invoked to explain the observed long-range migration. We first consider and eliminate the more common possible mechanisms, and end by offering a postulate, the validation of which requires a rigorous treatment of the adiabatic many-body potentials of the system.

First, we reject the possibility that the observed migration proceeds via defects, such as grain boundaries. Since all atoms are induced to thermally recombine, they would all have to be created in defects that percolate throughout the solid. Such a mechanism could be invoked in the case where O_2 is used as the O atom precursor, since in that case only a small fraction ($\sim 1\%$) is photodissociated, and may be suspected that the photodissociation proceeds at defect sites. However, the argument fails in the case of N_2O precursors, in which case the photodissociation is complete. Moreover, if the recombination were defect mediated, we would not expect reproducible and well defined peaks in the glow curves. This point was experimentally illustrated in the case of pulse deposited matrices, in which we clearly observe the effect of defects. Finally, we note that the experiments are conducted in highly transparent free standing crystals, which do not show any enhancement in optical scattering, either upon photodissociation or after subsequent thermal cycles.

Activated first order recombination is commonly encountered in the case of trapped charges due to band mobility.[25] The picture is one of a charge trapped in a localized gap state, just below the conduction band. The band is then thermally accessed, followed by coherent propagation of the delocalized charge. Attractive as this model is, it would be difficult to apply in the case of heavy particles, for which the de Broglie wavelength is much smaller than the lattice constant of the solid [at the temperatures of the present studies, $\hbar/(\mu kT)^{1/2} \sim 0.1$ d].

A second model to consider is one of a defect atom riding a ballistic phonon wave. At the temperatures at which recombination is observed, the mean free paths of thermal phonons are of order 30 Å ($\lambda = 3\kappa/Cv$; at 25 K, for Kr, the thermal conductivity $\kappa \sim 1$ $Wm^1\,K^{-1}$, $C \sim 0.22$ $Jg^{-1}\,K^{-1}$, $v = 1.38 \times 10^3$ ms^{-1}, and a molar volume of 0.325×10^{-3} $m^3\,kg^{-1}$).[26] The creation of phonons in the collisionless range, $\hbar\omega > k_B T$, is not possible since the observed migration temperatures are comparable to the Debye temperatures of the studied solids. Longer range mobility, limited by scattering from defects, could be expected for shock waves which may be generated during a recombination process, in which energies of order of the binding of O_2 of ~ 5 eV are generated. Ballistic propagation of such waves have previously been observed under similar conditions—induced by a sudden photodissociation process.[27] Such a mechanism may also be rejected, since it would lead to positive feedback, and thermal runaway, which is incommensurate with first order kinetics.

We postulate an alternate mechanism, one that involves thermal excitation of $O(^3P)$ to cross over to a singlet surface, and subsequent migration on the singlet surface until recrossing occurs. The diatomic O–Rg pair potentials immediately bring out this likelihood. As mentioned earlier, the $O(^3P)$–Rg interactions are essentially

repulsive, except for a small van der Waals minimum that occurs on the $^3\Pi$ surface, at 3.57 Å for Kr, and 3.69 Å for Xe.[26] $O(^1D)$–Rg interactions lead to three surfaces, the repulsive Δ and Π, and the bound $1\,^1\Sigma^+$ state.[28] The latter gains its binding character by mixing with $Rg^+O^-(^1\Sigma^+)$. While it has been difficult to characterize the $RgO(1\,^1\Sigma^+)$ state spectroscopically,[29] the *ab initio* calculations yield $D_e = 0.7$ eV and $r_e = 2.08$ Å for XeO, and $D_e = 0.25$ eV and $r_e = 2.0$ Å for KrO.[28] $O(^3P)$ may therefore be regarded to shrink by ~ 1.5 Å in diameter by becoming $O(^1D)$. Based on interaction radii alone, $O(^1D)$ is to be expected to be significantly more mobile. Based on the solvation of charge transfer configurations, an even deeper binding of this surface is to be expected. This has already been verified in the case of O/Xe, in which nearly doubling of the binding energy was observed.[1] Even more intriguing is the fact that we would anticipate very different minimum energy paths for motion on the triplet and singlet surfaces in a given lattice. While the ^3P atom, due to its repulsive potential, would occupy the largest cavities in the lattice, the ^1D atom would be expected to occupy the tighter sites, such as insertion between nearest neighbor Rg atoms. This would reduce the likelihood of recrossings, therefore retrapping, once the atom is activated to the singlet surface. This consideration, the absence of efficient retrapping, must be a feature of any model designed to explain the observed long-range mobility. Note, that the proper adiabatic surfaces arise from the spin–orbit coupled representation. In the coupled $|Jm_J\rangle$ basis, the $^3\Pi$ and $^1\Sigma^+$ pair potentials will mix and sustain an avoided crossing through the $\Omega = 0$ component. In the pair potentials, these interactions have been considered in some detail, since they are responsible for the quenching of $O(^1D)$ atoms by collisions with rare gases.[30,31] At the crossing points, $V_{s.o.} = \langle ^3\Pi | H_{s.o.} | ^1\Sigma^+ \rangle = 500\ cm^{-1}$ for XeO, and $200\ cm^{-1}$ for KrO.[30] Given the larger spin–orbit couplings in Rg^+ than in O, charge transfer configurations make a significant contribution to these splittings. With the lowering of ionic states by solvation in these polarizable solids, enhancement of the splittings should be expected. Moreover, in the many-body interactions, nearly additive contributions from neighboring atoms is to be expected. These combined effects, should result in significant lowering of the crossings. In this picture, passage over the crossing constitutes the activation of mobility, and long-range migration is expected to be the result of smaller periodic barriers for the "singlet" atomic configuration. A schematic of this postulated mechanism is illustrated in Fig. 10.

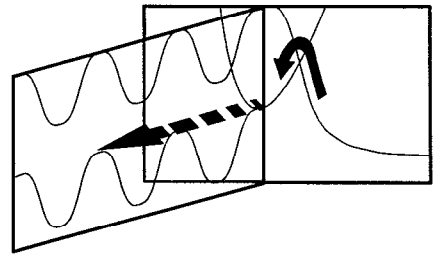

FIG. 10. Schematic of proposed migration mechanism. Thermal activation corresponds to spin conversion by passage over an avoided crossing. The singlet and triplet migration paths occur along different coordinates to avoid extensive retrapping. The potential energy modulation on the singlet surface is milder and should be possible to navigate by phonon assistance with little energy loss.

V. CONCLUSIONS

The thermally induced recombination between a random initial distribution of O atoms in crystalline Kr and Xe, at precursor dilutions as high as $\sim 1{:}30\,000$, proceeds with first order kinetics. This was demonstrated experimentally by three different measurements: Thermoluminescence from O_2, decay of LIF from atomic O during temperature ramps, and isothermal exponential decay of TL (i.e., of formation of O_2). All three measurements yield the same kinetics with identical rates. The implication of these observations is that the mobility of O atoms is characterized by long-range migration. A migration range of $\geqslant 300$ Å is estimated from the analysis of the recombination rate law as a function of O atom concentration. To rationalize this counter-intuitive result, it is suggested that the process may be compatible with an activation that corresponds to thermally induced triplet-singlet conversion, and subsequent phonon assisted migration on the singlet surface. To validate this hypothesis, scrutiny of the adiabatic potentials of this open shell atom interacting with many closed shell rare gas atoms is required. The minimal required features of such surfaces are: site specific activation barriers of order ~ 0.2 eV, and migration over a path that avoids extensive recrossing. The potentials should also be capable of reproducing the site specific emission spectra of atomic O.

Rather recently, Ryan and Weitz have observed that photoexcitation of O atoms in Xe matrices leads to long-range mobility.[12] The range of the observed mobility is quite comparable to the thermal mobility described in this paper. We have shown that indeed it is possible to photoactivate high energy traps, which can then migrate by the thermal rate constants of the low energy traps. It is therefore worth distinguishing between photon initiated mobility, in which the task of the photon is simply to activate the migration, and photomobility under conditions in which the atoms would be otherwise immobile (e.g., at temperatures below the thermal mobility onset). Mechanistically, the two processes can be quite distinct. In the case of thermal mobility, adiabatic dynamics controls the migration. In the case of photomobility, sudden dynamics prevails.

In the course of the mobility studies, we have also characterized the spectroscopy of O_2 trapped in Kr and Xe crystals. The spectroscopy in Kr is nearly identical to that of O_2 trapped in Ar, which has been reported in detail previously.[16,17] In the case of Xe, the excited triplet states of O_2 are strongly perturbed. The absence of fluorescence from these states may be due to incipient bonding along the O–Xe–O insertion coordinate. Details of the 193 nm photodynamics of O_2 is not fully understood. It is clear that partial dissociation occurs, leading to the formation of Frenkel defects: one O atom isolated in an interstitial site,

and another left behind in a substitutional site. In contrast, at 193 nm N_2O dissociates with nearly unit probability. The obvious difference between the two precursors is the fact that in the case of O_2, $O(^3P)$ atoms are generated, while in the case of N_2O photodissociation, $O(^1D)$ atoms are generated. As in the case of mobility, cage exit of the contracted $O(^1D)$ atoms should be subject to a negligible barrier. It was also noted, that initially N_2O photodissociation in Kr leads strictly to interstitial O atoms, and only subsequently do substitutional sites become occupied. This too is consistent with a doubly substitutional occupation site of N_2O, and subsequent lattice rearrangement induced by the photoexcitation of the O atoms.

ACKNOWLEDGMENT

This research was supported by the US Air Force Phillips Laboratory under Contract No. S04611-90-K-0035.

[1] W. G. Lawrence and V. A. Apkarian, J. Chem. Phys. **97**, 2224 (1992).
[2] H. Krueger and E. Weitz J. Chem. Phys. **96**, 2846 (1992).
[3] R. U. Taylor and W. C. Walker, J. Chem. Phys. **70**, 284 (1979).
[4] A. G. Belov, I. Y. Fugol, and E. M. Yurtaeva, Phys. Status Solidi B **175**, 123 (1993).
[5] K. Mahesh, P. S. Weng, and C. Furreta, *Thermoluminescence in Solids and Its Applications* (Nuclear Technology, Ashford, 1989).
[6] M. E. Fajardo and V. A. Apkarian, J. Chem. Phys. **89**, 4124 (1988).
[7] L. J. Schoen and H. P. Broida, J. Chem. Phys. **32**, 1184 (1959).
[8] J. Fournier, J. Deson, C. Vermeil, and G. C. Pimentel, J. Chem. Phys. **70**, 5726 (1979); J. Fournier, H. H. Mohammed, J. Deson, and D. Maillard, *ibid.* **70**, 39 (1982).
[9] J. Fournier, C. Lalo, J. Deson, and C. Vermeil, J. Chem. Phys. **66**, 2656 (1977).
[10] Y. P. Lee and G. Pimentel, J. Chem. Phys. **69**, 3063 (1978).
[11] W. G. Lawrence and V. A. Apkarian, J. Chem. Phys. **97**, 2229 (1992).
[12] E. T. Ryan and E. Weitz, J. Chem. Phys. (to be published).
[13] O. Schnepp and K. Dressler, J. Chem. Phys. **42**, 2482 (1965); E. Boursey, J.-Y. Roncin, and N. Damany, Chem. Phys. Lett. **5**, 584 (1970).
[14] J. Bahrdt and N. Schwentner, J. Chem. Phys. **85**(10), 6229 (1986).
[15] P. S. Julienne and M. Krauss, J. Mol. Spec. **56**, 270 (1975).
[16] A. C. Becker, U. Schurath, H. Dubost, and J. P. Galaup, Chem. Phys. **125**, 321 (1988).
[17] (a) J. Goodman and L. E. Brus, J. Chem. Phys. **67**, 1482 (1977); (b) R. Rossetti and L. E. Brus, *ibid.* **71**, 3963 (1979).
[18] A. V. Danilychev and V. A. Apkarian (unpublished).
[19] K. P. Crone and K.-J. Kügler, Chem. Phys. **99**, 293 (1985).
[20] J. L. Richards and P. M. Johnson, J. Chem. Phys. **65**, 3948 (1976).
[21] D. Maillard, J. Fournier, H. H. Mohammed, and C. Girardet, J. Chem. Phys. **78**, 5480 (1983).
[22] R. J. Chen, Appl. Phys. **40**, 570 (1969); J. Mater. Sci. **9**, 345 (1974).
[23] V. Aquilanti, R. Candori, and F. Pirani, J. Chem. Phys. **89**, 6157 (1988).
[24] See, for example, C. P. Flynn, *Point Defects and Diffusion* (Clarendon, Oxford, 1972), Chap. 11, and references therein.
[25] J. T. Randall and M. H. F. Wilkins, Proc. R. Soc. London Ser. A **184**, 347 (1945); **184**, 366 (1945); **184**, 390 (1945).
[26] V. A. Rabinovich, A. A. Vasserman, V. I. Nedostup, and L. S. Veksler, *Thermophysical Properties of Neon, Argon, Krypton, and Xenon* (Hemisphere, New York, 1987).
[27] H. Kunttu, J. Feld, R. Alimi, and V. A. Apkarian, J. Chem. Phys. **92**, 4856 (1990).
[28] T. H. Dunning, Jr. and P. J. Hay, J. Chem. Phys. **66**, 3767 (1977); **74**, 3718 (1981).
[29] J. D. Simons, A. G. Maki, and J. T. Hougen, J. Mol. Spec. **74**, 70 (1979).
[30] J. S. Cohen, W. R. Wadt, and P. J. Hay, J. Chem. Phys. **71**, 2955 (1979).
[31] S. R. Langhoff, J. Chem. Phys. **73**, 2379 (1980).